Available online at www.sciencedirect.com
SCIENCE DIRECT
Diamond & Related Materials 15 (2006) 1300 – 1309
DIAMOND AND RELATED MATERIALS
www.elsevier.com/locate/diamond

Osteoblasts attachment on amorphous carbon films

S.E. Rodil [a,*], C. Ramírez [a,b], R. Olivares [b], H. Arzate [b], J. Réyes-Gasga [c], C. Magaña [c]

[a] Instituto de vestigaciones en Materiales, Universidad Nacional Autónoma de México, Circuito exterior s/n, CU, 04510 México D.F., Mexico
[b] Facultad de Odontología, Universidad Nacional Autónoma de México, México D.F., Mexico
[c] Instituto de Física, Universidad Nacional Autónoma de México, México D.F., Mexico

Received 5 May 2005; received in revised form 1 October 2005; accepted 9 October 2005
Available online 28 November 2005

Abstract

In this work we studied the osteoblasts response to amorphous carbon (a-C) films deposited on stainless steel substrates with different surface textures. For osteoblasts cells, attachment to the substrate is the first step in the process of cell/surface interactions which affects subsequent cellular and tissue response. Amorphous carbon films are characterized by very smooth surfaces that imaged the surface roughness of the substrate and many of their applications rely on this property. However, in the biomedical field the cell response is strongly influenced by the topography and particularly, for osteoblasts cells it has been shown that rough surfaces enhances cellular attachment and differentiation. Therefore, in this work we modified the surface roughness of the substrate in order to obtain carbon films with different values of average surface roughness. The substrates were abraded or fine-polished to obtain four different average roughness: 0.01, 1.5, 2.1 and 3.5 μm. Surface topography before and after deposition of the a-C films was evaluated by profilometry and scanning electron microscopy (SEM), while chemical composition was determined by X-ray photoelectron spectroscopy. Human osteoblasts cells were used to evaluate the effect of the different surface finishes on the adhesion. The number of attached cells was determined by a colorimetric technique after 24 h of incubation, while morphological and cytoskeletal changes were monitored using SEM. The cellular attachment on a-C surfaces increases monotonically with the roughness attaining up to 160% more cells than the positive control.

Keywords: Amorphous carbon; Biomedical applications; Sputtering; Surface characterization

1. Introduction

The success of an implant is determined by its integration into the tissue surrounding the biomaterial. In the case of orthopedic or dental implants, it is essential to establish a mechanically solid interface with complete fusion between the material's surface and the bone tissue. Hence, a complete understanding of osteoblasts adhesion on materials is essential to optimize the bone/biomaterial interface that leads to successful bone formation. Bone formation, in vivo (osseointegration), requires recruitment of osteoblasts precursor cells, adhesion of the cells to the surface, proliferation, differentiation, production of unmineralized extra cellular matrix and calcification of the extra cellular matrix [1]. In vitro, these processes are studied by seeding the biomaterial surface with specific bone-forming cells to determine the ability of the cells to form calcium-phosphate minerals on the surface [2]. The first step of the cell–material interaction is the cellular adhesion process, which covers different phenomena. Firstly, the attachment phase which occurs rapidly and involves short-term events like physicochemical linkage between cells and materials and secondly, the adhesion phase occurring in the longer term and involving many biological proteins [3]. The proteins–surface interactions are dependent on the properties of both the proteins and the biomaterials surface. The most important surface properties are: geometric or morphological, chemical and electrical. For example, surfaces with more topographical features will expose more area for possible interactions with proteins, the chemical composition will determine which functional groups are available for interaction with the biomolecules and finally, surface potential influences the structure and composition of the electrolyte solution adjacent to the biomaterial. In vitro studies have demonstrated that for the osteoblasts cells there is a strong dependence of the cells–biomaterial interaction on the surface characteristics of the biomaterials, particularly the topography,

* Corresponding author.
E-mail address: ser38@zinalco.iimatercu.unam.mx (S.E. Rodil).

0925-9635/$ - see front matter © 2005 Elsevier B.V. All rights reserved.
doi:10.1016/j.diamond.2005.10.010

chemistry and surface energy [4,5]. Thus, different alterations of the biomaterials surface properties have been tried to improve the integration of the implants into the bone, such us: modification of the surface roughness [6,7], deposition of coatings to change the surface energy or the chemistry [8,9], ion implantation, etc.

In previous works [10,11], we studied the effect of depositing an amorphous carbon layer on stainless steel substrates to improve the biocompatibility and the mineralization process of stainless steel substrates. We showed that the amorphous carbon coatings did not exert any toxic effects for the osteoblasts cells, cells were able to adhere, proliferate and mineralize on the a-C surfaces. The mineralization was qualitatively better than in tissue plastic controls, but any attempt to compare the response between stainless steel, Ti and a-C coatings was influenced by the not uniform topography of the substrates [11,12]. Scanning electron images of the mineralization products showed that the distribution of the minerals was not uniform, and some mineral clusters were found associated to irregularities on the surface. In those works [10,11], no particular attention was put on the surface topography of the substrate, even though the effect of surface roughness on cellular response has been previously demonstrated for Ti implants [4,5,13,14]. Therefore, we concluded that in order to evaluate the osteoblasts response to the amorphous carbon coatings properly, surfaces with a uniform morphology should be used. On the other hand, it is well known that amorphous carbon films are characterized by very smooth surfaces that imaged the surface roughness of the substrate. Hence, the substrates should be previously modified to have a uniform morphology with a defined roughness before the deposition of the a-C films. From the literature, we found that atomically flat surfaces are of no interest, since osteoblasts-like cells attached significantly better on rough, sandblasted surfaces than on smooth surfaces [7,13]. Similarly, rough surfaces promote osteoblasts differentiation and mineralization [1]. Moreover, the optimum roughness value must be within a range that the cells can perceive, i.e. the roughness dimension need to be within the context of the cells size. With these ideas, we designed an experiment to evaluate the adhesion of osteoblasts cells on a-C surfaces having different roughness, ranging from 0.01 to ~4 μm. The roughness parameter used to characterize the surfaces was the average roughness, calculated as the arithmetic average of the absolute values of all points of a linear profile. The cellular response was compared to that obtained for the stainless steel substrate with similar roughness and a positive control consisting of plastic-culture plates.

The physical properties of amorphous carbon films deposited by magnetron sputtering have been extensively studied in the past [15–17]. They are characterized by a very small sp^3 fraction and a large clustering of the sp^2 sites, which leads to a small band gap and low hardness. Magnetron sputtering (MS) deposition is preferred for industrial applications because its versatility and its ease to scale up. The main disadvantage of the MS system for deposition of amorphous carbons is the relatively low ratio of energetic ions to neutral species. It is well known that the key property to produce hard amorphous carbon (Diamond-Like Carbon) is the ion bombardment, which promotes the formation of sp^3 bonding [18]. Thus, sputtered a-C films are not the hardest amorphous carbon films, they are mainly sp^2 bonded but differs from graphite due to the topological disorder. The biocompatibility of hydrogenated carbon (a-C:H) and tetrahedral amorphous carbon (ta-C) films have been documented using different in vitro and in vivo tests and a variety of cellular systems [19–22]. However, very few works have investigated the biocompatibility of a-C coatings. Particularly, we are interested on applications of the proposed substrate/coating system for orthopedic or dental implants and therefore it is important to study the interaction of the coating with human osteoblasts.

We also investigated the effect of roughness and composition on the wettability [23,24] and its subsequent relation with the cellular attachment, as it has been reported that high-energy surfaces (low contact angle) promote rapid cellular adhesion and spreading, whereas low energy surfaces do not [25].

2. Experimental

2.1. Preparation and characterization of the substrates

Commercial plates of stainless steel (SS) were cut into squares of 1 cm^2 area. To prepare the rough samples the squares surfaces were rubbed with abrasive particles (SiC with some Al_2O_3 particles as contaminants) of different grades. Grade C-120 produced a roughness of ~1 μm (sample M1), grade C-100 for ~2 μm (sample M2) and grade C-36 for ~3 μm (sample M3). Mirror polished samples (MP) were ground with SiC paper up to 1200 grade and then polished with diamond suspension (1/4 in.).

The average surface roughness, R_a, was measured using a profilometer (DEKTAK II). Two specimens of each sample (SSMP, SSM1, SSM2, SSM3) were randomly selected for recordings and up to six line scans of 1 mm length were made in opposite directions. The roughness was also measured after the a-C deposition (aCMP, aCM1, aCM2, aCM3) following the same procedure.

2.2. Coatings deposition

Prior to deposition, the substrates were ultrasonically cleaned in acetone for 30 min, followed by ultrasonic rinsing in isopropanol (30 min), then air-dried. A thin layer of Ti was deposited as a buffer layer to increase the adhesion between the amorphous carbon coating and the stainless steel substrate. The titanium layer was deposited by a pulsed magnetron sputtering system using argon as the precursor gas and a high purity Ti target. Amorphous Carbon films were deposited using a high purity hollow cathode graphite target in a dc magnetron sputtering system and argon plasma. The Ti/SS substrates were initially cleaned by an argon plasma for 10 min. The base pressure in the chamber was less than 2×10^{-4} Pa and the carbon films were deposited at 4 Pa using 0.4 and

argon flow-rate of 20 sccm for 5 min, leading to thickness of ~150 nm.

2.3. Cell culture

Human alveolar bone-derived cells (HABDCs) were obtained in the Odontological Department of the Universidad Nacional Autónoma de México by a conventional explant technique [26]. The cells were cultured in 75 cm^2 cell-culture flasks in a medium composed of Dulbecco's Modified Eagle's Medium (DMEM), supplemented with 10% fetal bovine serum (FBS) and antibiotic solution (Streptoycin 100 μg/ml and penicillin 100 U/ml, Sigma Chem Co.). The cells were incubated in a 100% humidified environment at 37 °C in an atmosphere of 95% air and 5% CO_2.

2.4. Cell attachment

Prior to cell seeding, all surfaces were sterilized by autoclave. The plastic-control was treated with poly-Lysine, protein that enhances cellular adhesion, and therefore was consider as a positive control to evaluate the percentage of cellular attachment. The a-C films and SS substrates were placed in 24-well culture plates, then the HABDCs were plated at an initial density of 1×10^4/well and left to adhere for 3 h. After this time, 500 μl of medium (DMEM supplemented with 10% FBS and antibiotic solution) were added. For quantitative attachment analysis, cells were incubated on each surface for 24 h by triplicate. After incubation, the unattached cells were removed with phosphate buffered saline (PBS) and the attached cells were fixed with 3.5% paraformaldehyde. Evaluation of cell attachment was performed by staining the fixed cells [27] with 0.1% toluidine blue during 3 h. Then, the dye was extracted with 0.1% of sodium dodecyl sulfate (SDS) and the optical absorption read with an ELISA (Enzyme Linked Immune Assay) micro-plate reader at 600 nm. The number of cells was then determined by correlating the absorbance of the experimental samples with the number of cells in a previously determined standard curve.

Cell morphology was evaluated by observing the cells using the scanning electron microscope, SEM, for different incubation periods: 30 min, 1, 4 and 24 h. At the end of the incubation time, the non-attached cells were removed by rising with PBS. Subsequently, cell fixation was carried out in 4% formaldehyde in 0.1 M phosphate buffer solution (pH 7.3), then dehydrated in 25%, 50%, 75% and 100% ethanol, and vacuum dried. A thin layer of gold was sputter-coated onto the samples before examination in a JEOL JSM 5600LV SEM at 20 kV.

2.5. Contact angle

Water contact angles were obtained using the sessile drop method with a Ramé-Hart Inc. system, model 100/07/00. Average values of the advancing angle, which were very similar to the receding angle, were obtained after 10 measurements. Although, it is usually stated that the difference between receding and advancing angle (hysteresis) should increase with the surface roughness, we did not observe any statistical difference or correlation between roughness and hysteresis in our data. This might be a consequence of the surface topography or the equilibrium conditions at which the measurements were made [28].

2.6. Composition

The surface chemical composition of the films was studied by XPS using a Thermo-Scientific Multilab, MgKα· radiation (1253.6 eV) operating at 3×10^{-9} mbar using a 500 μm spatial resolution and 50 and 20 eV pass energy for the survey and high resolution scan, respectively. These condition provide a full-width half maximum of 1 eV for the $Ag3d^{5/2}$ peak. Binding energy positions were calibrated using the main silver peak at 367.7 eV.

3. Results

3.1. Sample characteristics

3.1.1. Surface roughness

The results of the surface roughness for the SS substrates and the a-C coatings are shown in Table 1. The average roughness, R_a for the x and y directions were very similar, suggesting that the topography was isotropic in the plane. Comparing the roughness values before and after deposition, no strong differences were observed for the rough samples (M1, M2 and M3). However, for the mirror polished sample (MP) there was a small decrease in R_a (from 0.04 to 0.02 μm) after the coating deposition.

3.1.2. Morphology

SEM images of the eight surfaces are shown in Fig. 1. The left column shows the four SS surfaces and in the right column the surfaces after the a-C coating deposition. The mirror polished sample had the lowest level of visible roughness; the surface contained parallel grooves or scratches aligned in one direction. However, the profilometry tip could not detect any difference between the two directions, suggesting that the spacing between grooves was much smaller than the tip sharpness. The morphology of the roughed samples appeared to be quite similar, displaying dips and scratches randomly

Table 1
Surface average roughness, R_a, and standard deviations, σ, for the polished and roughed samples before and after film deposition

Sample	$R_a(x)$	σ	$R_a(y)$	σ
SSMP	0.042	0.008	0.044	0.012
SSM1	1.539	0.128	1.454	0.074
SSM2	2.143	0.141	2.201	0.094
SSM3	3.493	0.354	3.795	0.341
aCMP	0.018	0.005	0.020	0.005
aCM1	1.557	0.274	1.574	0.193
aCM2	2.284	0.150	2.268	0.270
aCM3	3.500	0.330	3.461	0.377

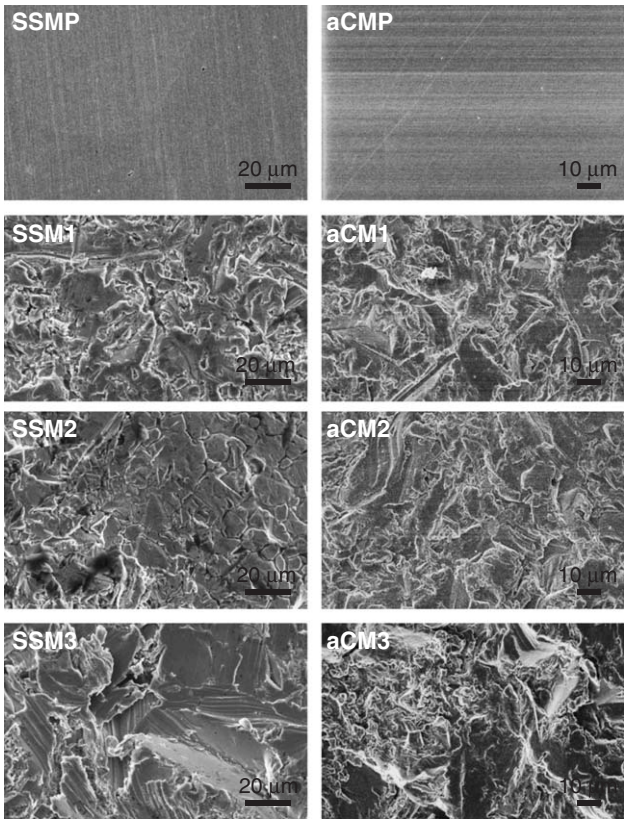

Fig. 1. Scanning electron microscopy photographs of the roughness surface of the samples. Stainless steel substrates are on the left, and a-C films on the right. The roughness magnitude is reported in Table 1 for each sample.

oriented. Analysis of the image using an image analysis software (Scion) showed that the three rough surfaces were completely isotropic, without any preferential orientation of the features. Comparing the images of the SSMP and the aCMP samples it might be seen that the decrease in average roughness measured with the profilometry could be explained by the coating coverage of the grooves.

3.1.3. Composition

Surveys and high resolution spectra of the four SS substrates are shown in Fig. 2. The signal to noise ratio for the rough samples is reduced, so the spectra are not of enough quality to estimate the composition, but allows us to compare the major elements present at the surface and any variation in their chemical environment. The survey spectra from the SS substrates (Fig. 2A) showed the presence of the major constituent elements of the alloy; Fe, O and Cr, carbon appears as both a constituent element and a surface contaminant, since no argon cleaning was used. The roughed samples showed the presence of Si and Al atoms that were incorporated during the roughening process, as was also confirmed by energy dispersive analysis with the SEM. High resolution spectra of the C, O and Fe signals (Fig. 2B,C,D) showed that there was a significant modification of the chemical state of the surface elements as a consequence of the roughening process. Analysing the spectra, we might say that as the roughness increases there was a reduction in the CrOx component with a subsequent increment in the FeOx and metallic Fe components. Moreover, the SSM3 sample pre-

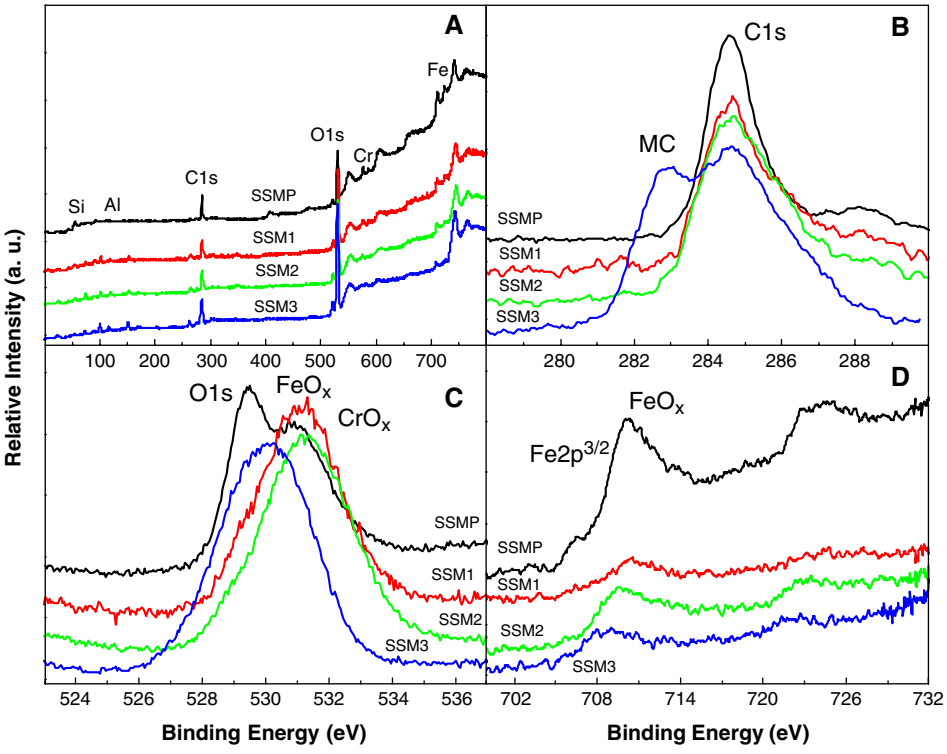

Fig. 2. (A) Typical XPS survey spectra of the stainless steel substrate for the four roughness. High resolution spectra of the main elements (B) C 1s, (C) O1s and (D) Fe $2p^{3/2}$.

sented the formation of metal carbides at the surface, suggesting that the CrOx was strongly substituted by CrC. This different chemical environment had some effect on the cellular response as shown later, but it could not be avoided since it is a natural consequence of the surface modification during the roughening process. The survey and high resolution spectra for the coated samples are shown in Fig. 3A and B. It might be seen that there are not Ti, Fe, Si, Cr or Al atoms on the surface, meaning that the carbon films covers completely the substrate and the Ti buffer layer, for any roughness. All the spectra were acquire without doing any argon cleaning of the surface, so there is approximately 12 at.% oxygen at the surface. It is not clear if the autoclave cleaning, made on the samples before cell seeding, removes this contamination or not, but it is important to see that no other elements from contamination were found. Fig. 3B shows the high resolution spectra of the carbon peak. Here we can see that the shape and position of the C1s peak for the four a-C samples were very similar, independently of the surface roughness. High resolution spectra were obtained to examine possible chemical shifts in the energy of the C1s photoelectron peak that could arise as a consequence of variations in the chemical state of the carbon atom. Thus, the results form Fig. 3B suggested that all the carbon samples have the same chemical state independently of the surface roughness, as expected since the deposition conditions were exactly the same.

3.1.4. Contact angle

Fig. 4 shows the decrease of water contact angle with roughness for the four stainless steel substrates and the coated substrates. These measurements were done to have an

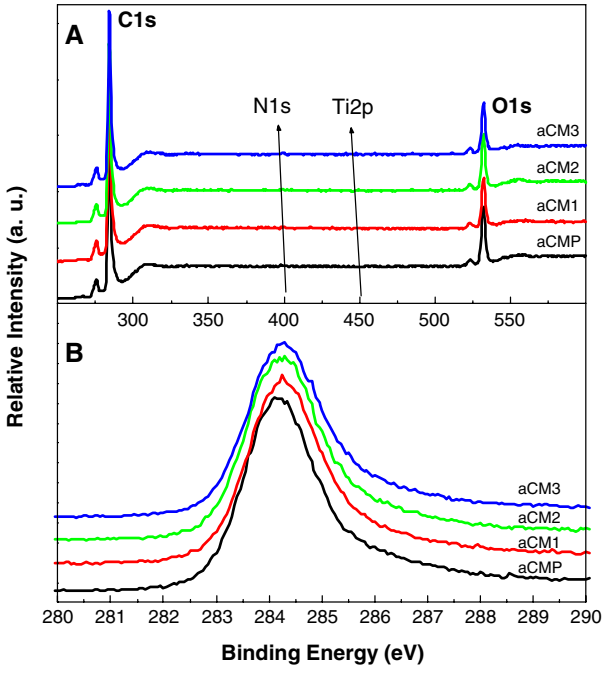

Fig. 3. (A) XPS survey spectra of the a-C films. Note that the unique surface contaminant is the oxygen, no other elements were detected. (B) High resolution spectra of the C 1s peak for the a-C films deposited on the rough SS substrates.

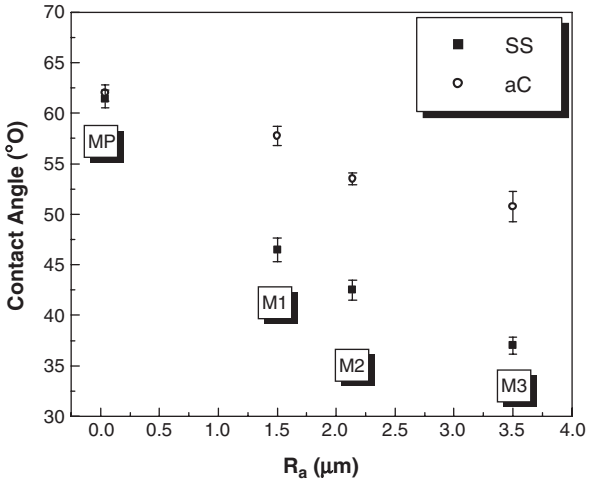

Fig. 4. Water contact angles as a function of the surface roughness for both SS substrates and a-C films.

insight into the hydrophilic or hydrophobic (wettability) character of the surfaces, since it has been shown to be an important parameter for cell adhesion [29,30]. A low contact angle indicates that the surface is hydrophilic and has a high surface energy. Conversely, a high contact angle means that the surface is hydrophobic and has a low surface energy. Cellular adhesion has been reported to occur preferentially to more hydrophilic surfaces for some materials, but this is just an empirical result valid for certain materials. Surface wettability in this model is modified by both the surface chemistry and the roughness. For the SS surfaces the water contact angle showed a strong decrease from 61.4±0.8 to 37±0.8. However, for the a-C coatings the variation was less pronounced from 62±0.8 to 50.7±1.5. We observed that as the SS surface becomes rougher, the wetting potential of the surface becomes higher. However, the variation in wettability for the coated substrates was smaller, even than the roughness variation was very similar, implying than other factors besides the surface roughness influence the wettability of the 316L stainless steel substrates. These factors could not be specifically determined in this work, but the chemical shifts observed in the XPS spectra suggested that the variations in the surface composition of the SS samples could be the cause of the strong variations obtained for the SS contact angles.

3.2. Cell number

Fig. 5 shows the percentage of attached cells for the a-C and the SS surfaces for each roughness. The percentage of attached cells was calculated assuming that the number of cells in the plastic control, after 24 h of incubation, corresponds to 100% attachment. For the carbon coatings the number of attached cells increases drastically with the roughness attaining up to 160% more cells than in the control. Meanwhile for the SS substrates the cell number remains nearly constant around 90%, showing no influence from the roughness. Cellular attachment is clearly enhanced in the amorphous carbon coating in

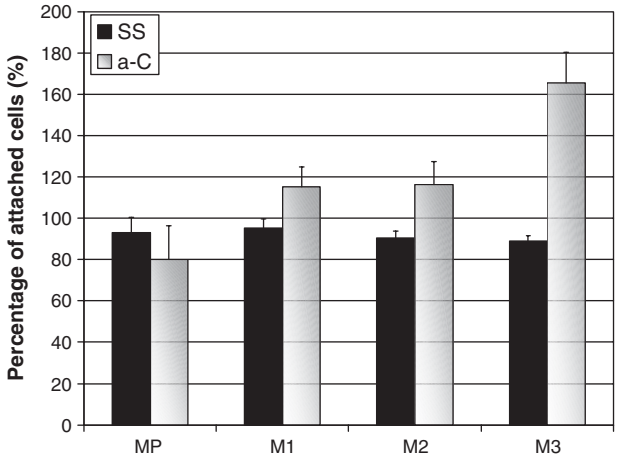

Fig. 5. Quantitative osteoblasts adhesion after 24 h, expressed as the percentage of attached cells in comparison with the plastic-positive control. Stainless steel substrates are compared with a-C films for the different roughness.

comparison with the SS substrate for roughness above 1 μm. This result is in agreement with our previous study of the biocompatibility of amorphous carbon coatings in which the cellular attachment was higher in a-C for both osteoblasts and fibroblasts cells than for metallic surfaces [10–12]. However, it is important to remark that the 90% of cellular attachment obtained for the SS substrates is a good indicator that the surface is not toxic to the cells. Any toxic effect should produce a decrease in the number of cells and this was also confirmed by performing viability assays (MTT test) on the surfaces (results not shown) [31].

3.3. Cell morphology

Fig. 6 shows the morphology of human osteoblasts cells cultured for 1 h on the carbon coated stainless steel. We did not observed any difference in the appearance of the cells due to the surface roughness. However, the cell shape was different depending on the chemical composition (carbon vs. steel) as shown later. The cells in Fig. 6 represented the initial stage of the adhesion with individual cells covering small surface area and not spreading. The osteoblasts were well attached to the substratum, so the lamellae, i.e. the membrane that extend from the cell and attach to the substrate, is not so obvious. Some pictures were taken at higher magnification and are presented in Fig. 7. Pictures 7B and C clearly showed the fillopodia (or microspikes) that precede lamellipodia and that lead to the formation of focal contacts. These structures anchor the cell and enable the cell to obtain traction as it spreads or migrates. Similar morphology was observed for 30 min, 2 and 4 h (not shown). It is after 24 h were a drastic variation in cell morphology was observed for the a-C coatings. Fig. 8 shows the cell morphology after 24 h for the a-C samples. It might be seen that at this time the HABDC have an elongated appearance covering long extensions (more than 10 μm), demonstrating a good state of adhesion and flattening to cover more surface area. In the rough samples (M1, M2, M3) cells are well spread with no preferred orientation, but for the aCMP sample the cells were oriented and elongated in the direction of the grooves. This is a well known phenomena called topographic or contact guidance that refers to the tendency of cells to be guided in their direction of locomotion by the shape of the substrate. In general, we observed that after 24 h the cells incubated on the carbon surfaces exhibited flattened, osteo-

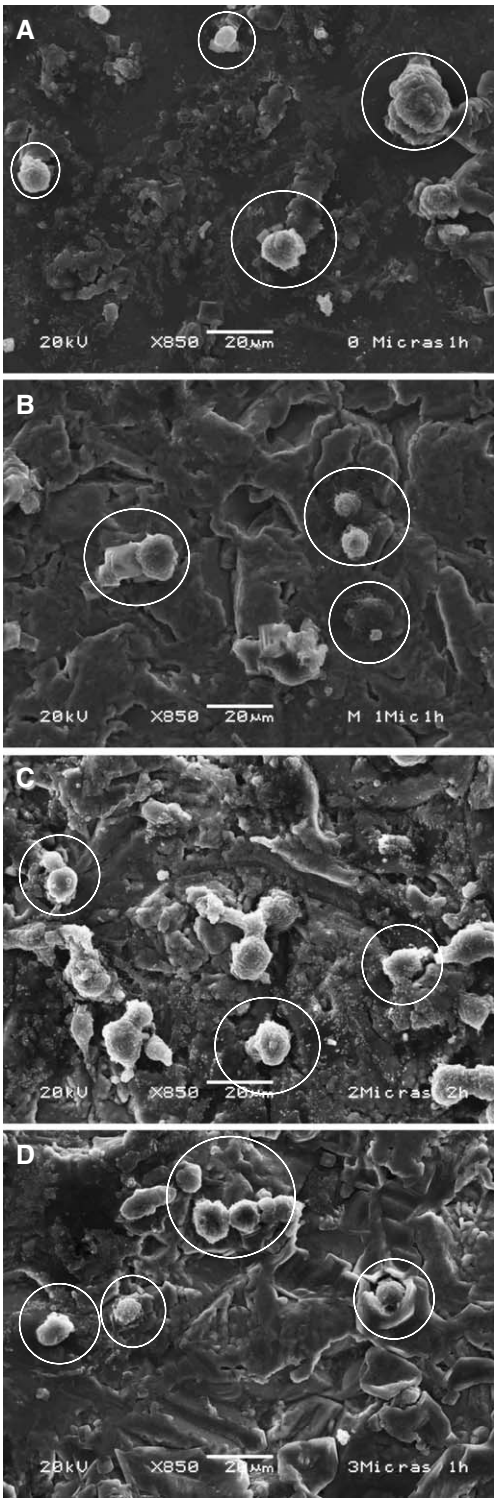

Fig. 6. SEM micrographs of human osteoblasts cultured on a-C films after 1 h of culture. (A) aCMP, (B) aCM1, (C) aCM2, (D) aCM3. The cells are in the first stage of adhesion covering small surface areas. Amplification: ×850.

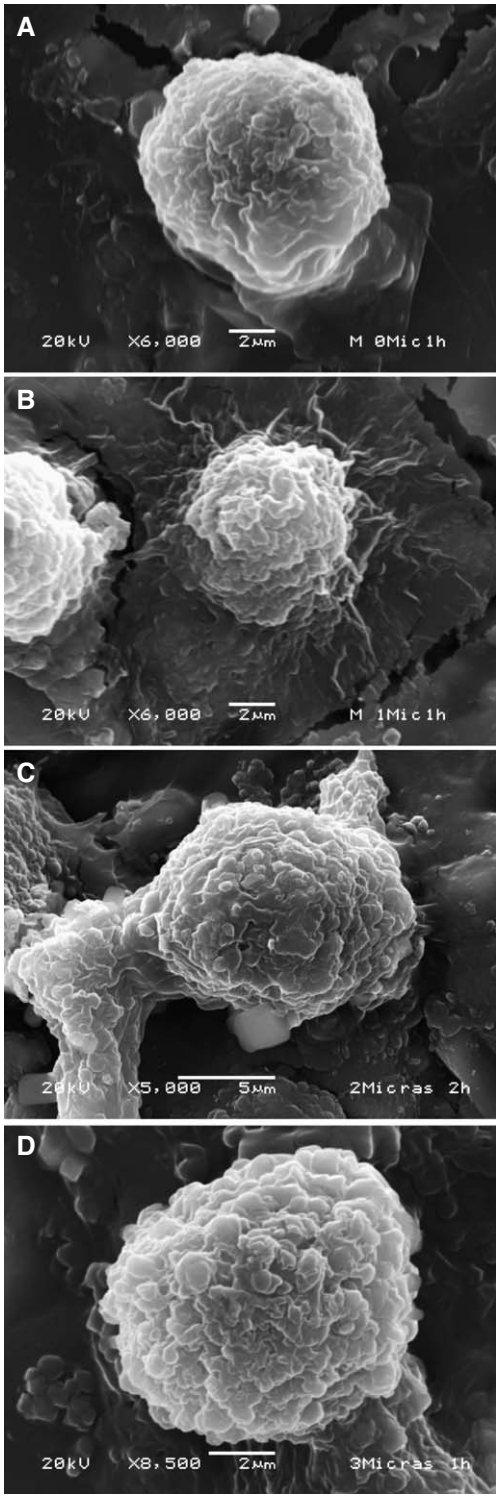

Fig. 7. Higher resolution images of the cells attached to a-C films after 1 h of culture. Cell morphology was similar for any roughness: rounded cells with development of fillopodia and lamellipodia around the nucleus.

blasts-like morphology, with cell processes attaching to the material surface.

Conversely, the morphology of the cells incubated in the SS substrates after 24 h was dramatically different. Fig. 9 shows this morphology for the different roughness. It might be seen that the cells presented only the morphology of the initial stage of adhesion, similar to that obtained for the a-C samples at 1 h of incubation. Fig. 9 shows the spherical nucleus with thin sheets of cytoplasm forming a well defined lamellipodia (*), indicating a good adherence to the surface but no spreading along the surface. The SEM images showed that there was a good cellular adhesion on all the SS surfaces. However, the

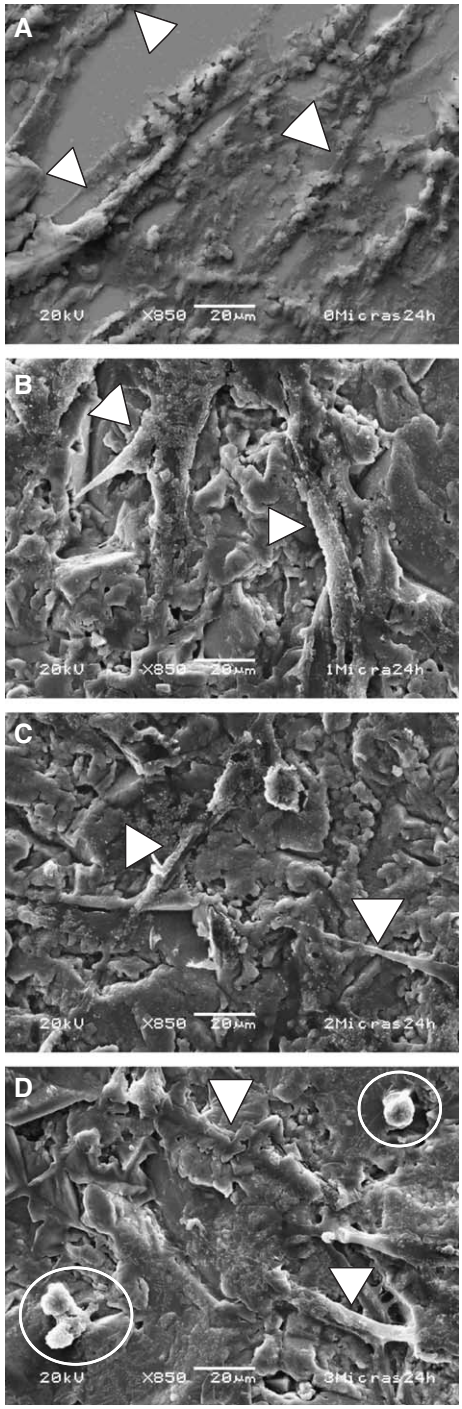

Fig. 8. SEM images of cells cultures on a-C films with different surface finishes after 24 h of incubation. (A) aCMP, note that cell's cytoskeletons are oriented parallel each other following the grooves left by the polishing process. (B) aCM1, (C) aCM2, (D) aCM3. The cells are flattened and spread along the surfaces without any preferential orientation. The triangles mark elongated cells, which are difficult to distinguish due to the surface topography.

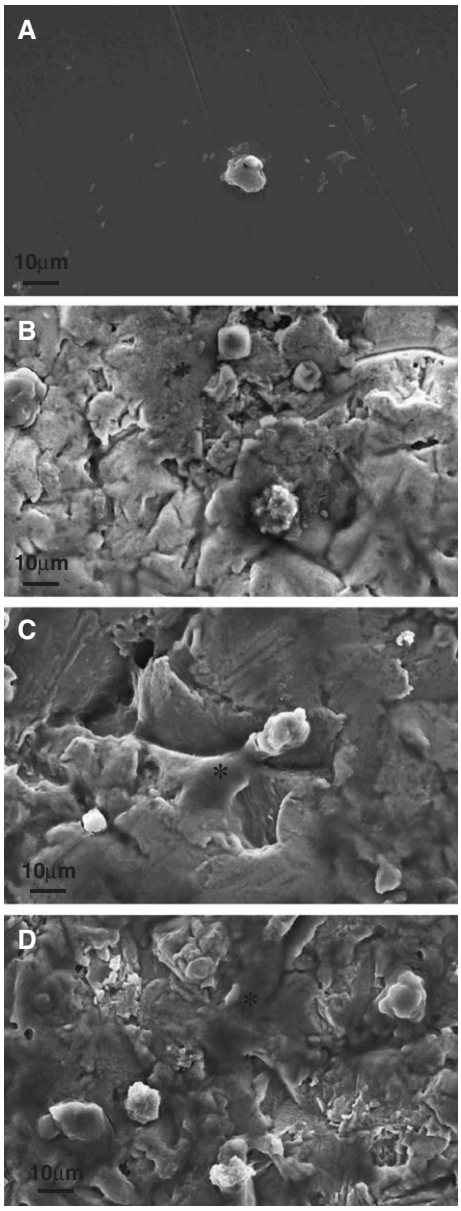

Fig. 9. Morphology of the human osteoblasts cells cultured on stainless steel substrates after 24 h. The magnification is ×850, (A) SSMP, (B) SSM1, (C) SSM2, (D) SSM3. Note that cells are still in the initial stage of adhesion; rounded and without spreading onto the surfaces, as observed for the a-C surfaces after 1 h. The (*) marks the lamellipodia, which looks as shadow around the cell nucleus.

cellular adhesion and spreading was not enhanced by the surface roughness, as observed for the a-C samples. This might be a consequence of the variation in the surface composition of the stainless steel samples as the roughness was increased and qualitativeley detected by the XPS spectra.

4. Discussion

The initial attachment of bone cells to the surface of an implant material define the subsequent events, such us, cell proliferation, matrix formation, cell differentiation and mineralization. Most cells need to attach to the substratum to grow and proliferate, and, in many cases, even to survive. This is a complex process, which is mainly mediated by proteins and the intracellular signals they generate. Which protein adsorbs to the surface and their signals are influenced by the topography and physicochemical properties of the surface. Some proteins present in the plasma, blood, saliva, extracellular fluid or in cell culture media are adsorbed in the surface and then interact with the proteins of the cell, defining an specific cellular response. The initial cellular response is the organization of the cytoskeleton whose function is to adhere the cell to the substrate through the formation of fillopodia and lamellopodia and the subsequent migration of the cells to colonize the surface. The physical spreading of a cell on the surface has a strong influence on intracellular events. Indeed, cells that are force to spread over a large area survive better and proliferate faster than cells that are not spread out. This stimulatory effect of cell spreading presumably help tissues to regenerate after injury. However, the mechanism and factors influencing how the cells sense its extent of spreading are still uncertain. It is only during the last decades that all this phenomena has been elucidated, therefore there is very few information about the specific effects of the physiochemical properties and surface topography on the cellular response. In this work, we have investigated two surfaces having different properties but similar topographies and the experimental results demonstrated a different cellular response, in terms of cellular organization and number.

Amorphous carbon coatings have shown to be a good candidate for biomedical applications, their chemical properties clearly induce osteoblasts cells to attach and proliferate. Previous characterization of the a-C coatings demonstrated that it is a low bandgap semiconductor [10], while the stainless steel substrates are metallic. We observed that at roughness lower than 1 μm the number of attached cells was very similar (not statistical difference could be established) for both the aCMP and the SSMP surfaces. Nevertheless, the cell morphology was different, cells spread more faster in the a-C coatings than in the SS substrates. For roughness above 1 μm, both the percentage of attached cells and the cell morphology were markedly different among the two surfaces. The degree of cell colonization and spreading after 24 h was rather different; in a-C the cells were spread along the surface and showed an elongated shape for any roughness, while in the metallic surfaces the cells show a rounded morphology with minimal cell colonization. The reasons for this difference can only be speculated in terms of a different protein adsorption and cell signaling due to the different surface properties. For the a-C samples, the surface composition was the same independently of the roughness and in consequence the surface morphology and the variation in the wettability enhanced the cell organization, leading to a large number of attached cells and surface colonization. On the other hand, for the SS substrates some differences in the surface composition could be detected, which could explain the different cell response. The results of the in-vitro model used in this work indicated that human osteoblasts cellular adhesion and spreading is enhanced in rough a-C coatings and therefore we expect a better cellular

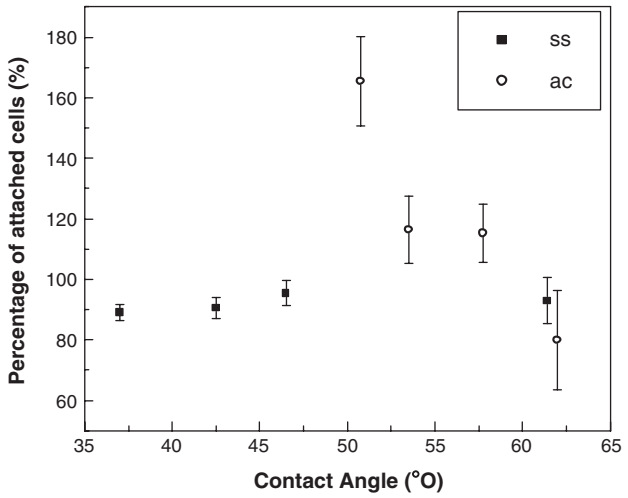

Fig. 10. Cell adhesion as a function of the water contact angle for both SS and a-C surfaces.

proliferation and differentiation. Further studies must be realized to confirm this hypothesis.

The effect of wettability on the cellular adhesion is more difficult to evaluate. Surface roughness affects wettability in different ways depending on the topographical features, and wettability is one of the most important parameters when biomaterials for implant devices are designed. In this work, we observed that increasing surface roughness leads to a decrease in the water contact angle, for any surface (a-C or SS). The variation was stronger in the metallic surfaces than in a-C, but in both cases the rougher samples exhibited the smaller contact angles. This is indeed not a common result, since it is more frequent to observe an increase in the water contact angle, or a lower wettability, as the surface roughness is increased [32]. However, the dependence of wettability on surface roughness is not straightforward and it is strongly influence by the particular topography. Thus, in our case, the topography produced by the roughening process induces an increase of the wettability as the average surface roughness increases. Similar results were observed for SS surfaces when a chromosulfuric acid method was used to increase the surface roughness [33] or by mechanical roughening [34].

A large number of research groups have studied the effect of substrate wettability on the interactions of biological species with solid substrates. Most groups [35–37], however, have studied the interactions of cells with polymeric substrates and very few data concerning other materials have been published. For the polymeric materials, results using wettability gradients suggested that cells adhere better on the moderately wettable surfaces having water contact angles around 55–60°. Similarly, cells were more spread onto the sections with moderate hydrophilicity (55°) than more hydrophilic sections (48°) and not spreading was observed for the hydrophobic section (98°). This is explained in terms of a surface-hydrophilicity-induced change in the adsorbed proteins. Therefore, assuming a similar response we would expect that contact angles between 50° and 60° presented the higher cellular attachment and spreading. Fig. 10 plots the percentage of attached cells versus the water contact angle. For the a-C surfaces, we observed a larger number of cells attached to the M3 sample having a water contact angle around 50° and corresponding to the rougher sample. However, for the metallic surface the cellular attachment is nearly independent of both wettability and roughness, which could be an indication that, under the present conditions, the surface composition played a more important role.

5. Conclusions

The interactions of different type of cells with various solid substrates depend mainly on surface characteristics such us wettability, chemistry, charge and roughness. In this paper, we focused on the relation between cellular attachment and roughness of the amorphous carbon coatings. To produce different topographies stainless steel substrates were modified by a grit-blasting process and the films were then deposited by magnetron sputtering. After characterizing the roughness, wettability and composition of the SS substrates and the a-C coated samples, osteoblasts attachment assays were carried out to correlate average roughness and the amount of cellular attachment. The results obtained suggested that there was a synergistic effect between composition and roughness that allows a higher percentage of cellular attachment on the amorphous carbon coatings. SEM observation of the cell morphology also verified that the cells spread better onto the amorphous carbon coatings than in the metallic substrates, independently of the roughness. However, in the stainless steel substrates the roughening process modified the composition to such a extent that neither the modification of the surface roughness or wettability were able to enhance the cellular attachment. These results will be used to continue the investigations about the biomineralization on amorphous carbon coatings, but further investigations will be concentrated on a-C coatings having average roughness above 2 μm instead of working on polished samples.

Acknowledgements

L. Huerta for XPS measurements and A. Ordoñez for her assistance with the contact angle measurements. S.E. Rodil acknowledges economical support from DGAPA-PAPIIT projects IN100701 and IN100203.

References

[1] B.D. Boyan, Z. Schwartz, in: J.E. Davies (Ed.), Bone Engineering, EM Squared, Toronto, 2000, p. 232.
[2] B. Groessner-Schreiber, R.S. Tuan, J. Cell Sci. 101 (1992) 209.
[3] K. Anselme, Biomaterials 21 (2000) 667.
[4] J. Lincks, B.D. Boyan, C.R. Blanchard, C.H. Lohmann, Y. Liu, D.L. Cochran, D.D. Dean, Z. Schwartz, Biomaterials 19 (1998) 2219.
[5] B. Chehroudi, D.M. Brunette, in: D.L. Wise (Ed.), Biomaterials and Bioengineering Handbook, Marcel Dekker, New York, 2000, p. 813.
[6] G. Lauer, M. Wiedmann-Al-Ahmad, J.E. Otten, U. Hubner, R. Schmelzeisen, W. Schilli, Biomaterials 22 (2001) 2799.
[7] E. Conforto, B.-O. Aronsson, A. Salito, C. Crestou, D. Caillard, Mater. Sci. Eng., C, Biomim. Mater., Sens. Syst. 24 (2004) 611.

[8] L. Montanaro, C.R. Arciola, D. Campoccia, M. Cervellati, Biomaterials 23 (2002) 3651.
[9] M.H. Prado da Silva, G.D.A. Soares, C.N. Elias, S.N. Best, I.R. Gibson, L. Disilvio, M.J. Dalby, J. Mater. Sci. Mat. Med. 14 (2003) 511.
[10] S.E. Rodil, R. Olivares, H. Arzate, S. Muhl, Diamond Relat. Mater. 12 (2003) 931.
[11] S.E. Rodil, R. Olivares, H. Arzate, Biomed. Mater. Eng. 15 (2005) 101.
[12] R. Olivares, S.E. Rodil, H. Arzate, Surf. Coat. Technol. 177–178 (2004) 758.
[13] B.D. Boyan, S. Lossdorfer, L. Wang, G. Zhao, C.H. Lohmann, D.L. Cochran, Z. Schwartz, Eur. Cells Mater. 6 (2003) 22.
[14] R.K. Sinha, F. Morris, S.A. Suken, R.S. Tuan, Clin. Orthop. Relat. Res. 305 (1994) 258.
[15] J.J. Cuomo, J.P. Doyle, J. Bruley, J.C. Liu, Appl. Phys. Lett. 58 (1991) 466.
[16] G.M. Pharr, D.L. Callahan, S.D. McAdams, T.Y. Tsui, S. Anders, A. Anders, J.W. Ager, I.G. Brown, C.S. Bathia, S.R.P. Silva, J. Robertson, Appl. Phys. Lett. 68 (1996) 779.
[17] S. Logothetidis, Appl. Phys. Lett. 69 (1996) 158.
[18] J. Robertson, Mater. Sci. Eng. R 37 (2002) 129.
[19] L.A. Thomson, F.C. Law, N. Rushton y, J. Franks, Biomaterials 12 (1991) 37.
[20] R. Butter, M. Allen, L. Chandra, A.H. Lettington y, N. Rushton, Diamond Relat. Mater. 4 (1995) 857.
[21] M.I. Jones, I.R. McColl, D.M. Grant, K.G. Parker y, T.L. Parker, J. Biomed. Mater. Res. 52 (2000) 413.
[22] M. Allen, B. Myer, N. Rushton, J. Biomed. Mater. Res. 58 (2001) 319.
[23] Y. Tamai, K. Aratani, J. Phys. Chem. 76 (1972) 3267.
[24] C. Della Volpe, D. Maniglio, M. Morra, S. Siboni, Colloids Surf., A Physicochem. Eng. Asp. 206 (2002) 47.
[25] S.H. Hsu, Biomaterials 21 (2000) 359.
[26] H. Arzate, M.A. Alvarez-Pérez, M.E. Aguilar-Méndoza, J. Peridontal Res. 33 (1996) 390.
[27] G. Hayman, E. Engvall, E. A'Hearn, J. Cell Biol. 95 (1982) 20.
[28] C. Della Volpe, D. Maniglio, M. Morra, S. Siboni, Colloids Surf., A Physicochem. Eng. Asp. 206 (2002) 47.
[29] L. Weiss, Int. Rev. Cyt. 9 (1960) 187.
[30] L. Ponsonnet, K. Reybier, N. Jaffrezic, M. Lissac, C. Martelet, Mater. Sci. Eng., C 23 (2003) 551.
[31] S.E. Rodil, R. Olivares, H. Arzate, S. Muhl, in: G. Messina, S. Santangelo (Eds.), Springer Series Topics in Applied Physics, pp. 5171. To be published.
[32] R.N. Wenzel, J. Phys. Colloid Chem. 53 (1949) 1466.
[33] H.P. Jenninsen, Biomaterialien 2 (2001) 45.
[34] L. Hao, J. Lawrence, Y.F. Phua, K.S. Chian, G.C. Lim, H.Y. Zheng, J. Biomed. Mater. Res. Part B: Appl. Biomater. 73B (2005) 148.
[35] K.H. Kim, J.S. Cho, D.J. Choi, S.K. Koh, Nucl. Instrum. Methods Phys. Res., B 175–177 (2001) 542.
[36] E.A. Vogel, R.W. Bussian, J. Biomed. Mater. Res 21 (1981) 1197.
[37] H. Lee, J.W. Park, H.B. Lee, Biomaterials 12 (1991) 443.